Proceedings of ASME Turbo Expo 2011
GT2011
June 6-10, 2011, Vancouver, British Columbia, Canada

GT2011-46272

PERFORMANCE ANALYSIS OF A 565 MW STEAM POWER PLANT

R. Chacartegui, D. Sánchez, J.A Becerra, A. Muñoz, T. Sánchez

Thermal Power Group (GMTS)
Escuela Técnica Superior de Ingenieros
Camino de los descubrimientos s/n
41092, Sevilla, Spain
Email: ricardo/davidsanchez/jabv/ambl/tmsl@esi.us.es

ABSTRACT

In this work, a tool to predict the performance of fossil fuel steam power plants under variable operating conditions or under maintenance operations has been developed. This tool is based on the Spencer-Cotton-Cannon method for large steam turbine generator units.
The tool has been validated by comparing the predicted results at different loads with real operating data of a 565 MW steam power plant, located in Southern Spain. The results obtained from the model show a good agreement with most of the power plant parameters.
The simulation tool has been then used to predict the performance of a steam power plant in different operating conditions such as variable terminal temperature difference or drain cooler approach of the feed-water heaters, or under maintenance conditions like a feed-water heater out of service.

1. INTRODUCTION

An accurate prediction of the performance of a power plant, with the corresponding detailed evaluation of its thermodynamics variables, allows to avoid undesirable or abnormal operating conditions or to anticipate solutions to certain unusual operating conditions like those derived from maintenance labours.
In this regard, the present work focuses on the estimation of the part load operation of a fossil fuel steam power plant, making use of well known reference models. The tool so developed is then used to estimate power plant performance under several operating circumstances. More in particular, this tool is based on several ASME papers developed by engineers of General Electric. The original work was developed by Warren and Knowlton in 1940 [1] with the aim of predicting the performance of large steam generator-alternator units without reheating, and has been periodically revised later. Thus, Elston and Knowlton [2] incorporated reheat units into the possible plant configurations and, later, Hegetschsweiler and Bartlett [3] extended the design method for partial loads in 1956.
Nevertheless, the most important update to this method was written in 1962 by Spencer, Cotton and Cannon [4] who later revised it in 1974 incorporating the most recent technological developments at that time. This methodology has been used ever since its publication as the basis to calculate the performance of large steam turbine units, even if some modifications have been incorporated by different authors.
In essence, the Spencer, Cotton and Cannon (SCC) method is based on empirical data with respect to which correlations or fitting curves are developed. These curves are later applied to the calculation of heat and mass balances of the plant, making use of the necessary correction factors depending on the configuration and specific features of the system (mostly working cycle).
As indicated by Hegetsweiller and Bartlett [3], a large steam turbine can be considered as a series of relatively independent turbine segments, and its performance as a single component can be derived from the evaluation of each individual stage. Such stage by stage calculation methods are appropriate for evaluating existing turbine designs for which almost complete information of turbine characteristics exists. However, for predicting the performance of new units in a design step or when in an operating power plant some of the turbine data are unavailable, the stage by stage method is not valid. In these cases the GE method is useful, as it gives a good approach for evaluating the efficiency.

2. REFERENCE PLANT

The methodology outlined in the previous section, and described in detail later, is applied to the default power plant

 Copyright © 2011 by ASME

shown in Figure 1. The layout in this figure can be taken as typical of large coal power plants and will hence be used as reference.

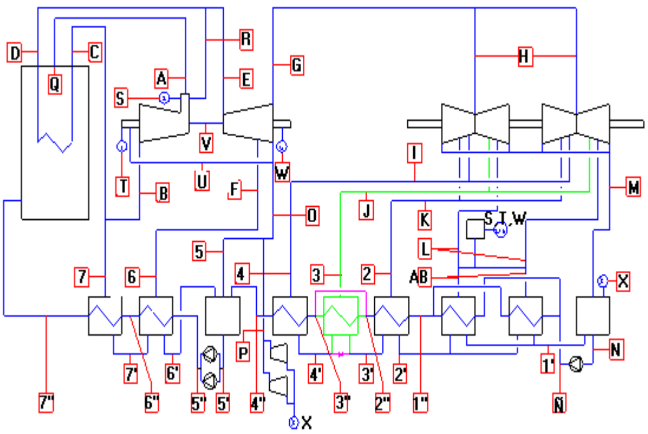

Figure 1. Layout of reference power plant.

In summary, the reference power plant is based on a reheat Rankine cycle with seven feedwater heaters, four of which are of the low-pressure type. The turbine comprises independent high pressure and intermediate pressure sections and a multiple-flow low pressure assembly, all mounted in a tandem-compound configuration (single-shaft). The condenser is of the water-cooled direct type and the feedwater pump is turbine-driven. Finally, the electric generator is air-cooled and directly driven by the turbine assembly. More specifications of the real power plant used for validation are provided later in Section 7.

3. CALCULATING EFFICIENCY

3.1. Rated efficiency

The full-load or rated performance of a steam turbine can be obtained if the following data are known:

1. Stage efficiency. It can be obtained from volumetric flow, pressure ratio, inlet conditions (pressure and temperature) and governing stage design (if any).
2. Exhaust losses.
3. Tip leakage losses.
4. Interstage packing leakage losses.
5. Mechanical losses.
6. Generator-alternator electrical and mechanical losses.

Items 1 to 4 provide the internal or isentropic efficiency of the unit, which is applied to the isentropic enthalpy drop (from inlet pressure and temperature before the stop-valve to exhaust pressure) to calculate the gross mechanical output or shaft work. Items 5 and 6 are later applied to previous shaft work to calculate the gross electrical output at generator terminals, thus yielding a global electrical efficiency of the turbine.
The on-design efficiency of each turbine section is calculated from the recommendations given by SCC directly and summarised in Table 1. This table is excerpted from references [4,5] and provides a set of base values and corrections factors whose analytical expressions are listed in the Appendix to this article. There are other approaches available, amongst which the method described by Schegliaiev in reference [6] is of special interest. This "detailed" method is based on a stage-by-stage calculation of turbine efficiency and therefore requires a significant amount of data regarding stage design. Thus, even though both approaches emerge from the common source of Stodola's work [7] and have many similarities, the former method is preferred. The rated efficiencies so calculated are: 80.74% HP and 91.58% IP/LP.

3.2. Part-load efficiency

At partial loads, stage efficiencies hardly change from the governor stage down to the last few stages before the low pressure turbine exhaust, due to their almost constant expansion ratio. Therefore, the part-load efficiency curves of IP stages remains rather flat whereas in high pressure stages (HP) with throttle control, the efficiency is mainly a function of the inlet volumetric flow ratio yielding decreasing efficiencies for decreasing mass flows [6-8]. The efficiency of low pressure sections (LP) mostly depends on the axial velocity of steam leaving the last stage exhaust hood, which is the main parameter affecting kinetic energy losses (namely velocity losses) and, to a lesser extent, leakage losses.
Sample plots of part-load efficiency for a heavy duty high-pressure steam turbine with valve control are shown in Figure 2 for both approaches. It is observed that even though SCC's method overestimates efficiency by two to three percentage points with respect to Schegliaiev's, the slope of both curves is the same.

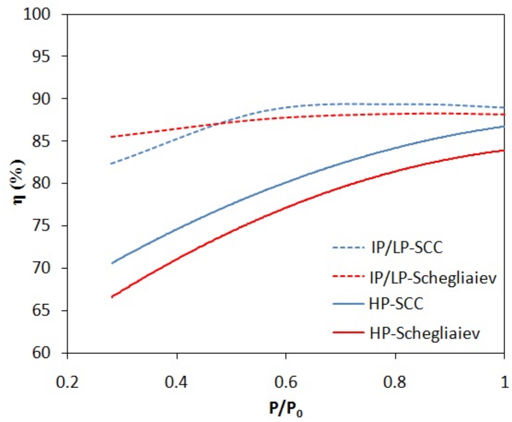

Figure 2. Part-load efficiency of HP and IP/LP sections.

The plots shown in Fig. 2 have been obtained from the same input data of a reference steam turbine whose complete stage-by-stage geometry is known a priori. It is worth noting that Schegliaiev's approach cannot be used unless this information is available, which is not the case most of the times. Otherwise the method is not usable and the more general SCC's approach must be employed. This is the main reason why the case study presented in this work makes use of the latter method to estimate turbine efficiency.

Copyright © 2011 by ASME

High pressure (HP) section

The expansion line of reheat high pressure sections can be thus considered as a straight line, starting from throttle enthalpy and a pressure slightly lower than throttle pressure to account for inlet losses. The expansion line end point (ELEP) is calculated by means of the turbine section efficiency which is updated for part-load operation as illustrated in Fig. 2 (using whichever method). Then, an expansion line parallel to the previous design case is drawn, starting from the new ELEP.
Expansion lines for both cases, full and part-load operation, are shown in Fig. 3 (left).

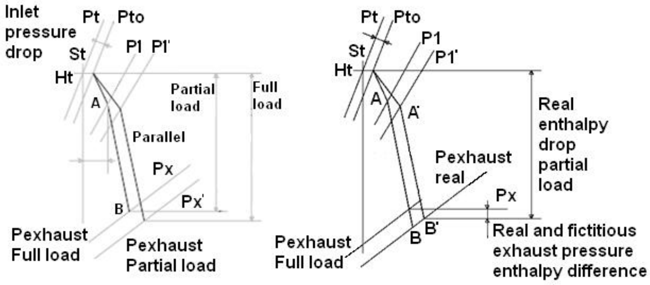

Figure 3. Partial load expansion: HP (left) and non-reheat (right) sections.

Intermediate/low pressure (IP/LP) section

In condensing steam turbines, the internal efficiency estimated from SCC's or Schegliaiev's methods is applied to the available isentropic enthalpy change from the conditions before the hot reheat intercept valve to a reference condenser pressure of 0.05 bar. Then, a differential enthalpy is added/detracted to account for the real condensing pressure and a correction for moisture is applied. Thus, the real ELEP is obtained and the expansion line can be plotted from the latter point up to the inlet conditions before the intercept valve. Unlike the previous case of high pressure sections, the expansion line of an IP/LP section cannot be considered a straight line. Instead, a variable slope line must be used that incorporates the negative effect of moisture on efficiency. Keuffel and Esser Curve No. 1864-31 can be used to this aim for the vast majority of intermediate/low pressure sections of large steam turbine generators as reported in [3].

3.3. Exhaust losses

Exhaust losses account for the leaving kinetic energy of steam at the exhaust hood of the low pressure turbine. This energy is not recovered downstream of the LP section and therefore is considered an additional loss when defining the isentropic (total to static) efficiency.
Exhaust losses depend on the annular velocity of exhaust steam which depends itself on mass flow rate, pressure, moisture and annulus area at turbine exhaust (the number of LP flows must also be considered). Experimental information, as available in reference [4] or similar, is generally used to estimate kinetic energy losses.
With this information, the so called Used Energy End Point (UEEP) can be evaluated. The enthalpy change from IP turbine inlet ahead of the intercept valve to the UEEP yields the gross specific work of the IP/LP section:

$$ELEP_{p_c} = ELEP_{1.5''} + \Delta ELEP_{Y=0}(0.87)(1-0.01Y)(1-0.0065Y) \qquad \text{Eq. (3)}$$

$$UEEP = ELEP_{p_c} + EL(0.87)(1-0.01Y)(1-0.0065Y) \qquad \text{Eq. (4)}$$

$$EL = f(V_{an}) = f\left(\frac{Q\cdot v\cdot(1-0.01Y)}{A_{an}}\right) \qquad \text{Eq. (5)}$$

$$W_{IP/LP} = h_{IP,in} - UEEP \qquad \text{Eq. (6)}$$

It is worth noting that even though the UEEP (stagnation exhaust point) is used to calculate the specific work generated by the turbine, the enthalpies of steam extractions are taken

Turbine type	HP Sections		IP Sections	Reheat Sections		
	60 Hz Non Condensing 1-Row GS	60 Hz Non Condensing 2-Row GS	60 Hz Non Condensing No GS	60 Hz Condensing No GS	60/30 Hz RPM Condensing No GS	30 Hz Condensing No GS
Base Efficiency	87%	84%	CF#13	91,93%	91,93%	92,95%
Δη for volume flow	Reduce in (%) $\frac{126.7445511\cdot N}{Q_v}$	Reduce in (%) $\frac{170.22\cdot N}{Q_v}$		Reduce in (%) $\frac{160.1328889\cdot N}{Q_v}$	Reduce in (%) $\frac{160.1328889\cdot N}{Q_v}$	Reduce in (%) $\frac{160.1328889\cdot N}{Q_v}$
Δη for governing stage	CF#7					
Δη for pressure ratio	CF#6	CF#10				
Δη for initial conditions				CF#14	CF#14	CF#14
Δη for partial load in a GS	CF#8					
Δη for partial load	CF#9	CF#11				
Δη for substitution of 30 Hz LP section.					Increase in (%) $1.25\left(\frac{\Delta h_{1800}}{\Delta h_{reheat}}\right)_{1.5''}$	
Δη for the admission throttle flow.	CF#12	CF#12				

Table 1. Efficiency Calculation [4,5].

Copyright © 2011 by ASME

from the expansion line that ends in the ELEP (static exhaust point).

3.4. Generator losses

Generator losses depend on the cooling system, rotating speed and power output of this equipment and include all the electrical and mechanical losses of the electrical generator and turbine coupling except bearing looses, accounted for in the turbine mechanical losses. The two correction factors K_1 and K_2 listed in Table A2 of the Appendix are used to estimate generator losses:

$$Gen_{loss} = MVA_{rated} \cdot \frac{(MW_{actual}/PF)}{MVA_{rated}} \left(\frac{K_1 K_2}{100}\right) \quad \text{Eq. (7)}$$

The mechanical losses of the turbine are constant for a given turbine-generator set and rotating speed.

4. CALCULATING MASS FLOW RATES

4.1. Inlet and drain steam flows of feedwater heaters

The amount of steam extracted from the turbine to preheat the feedwater depends on the enthalpy of steam, the mass flow rate of feedwater and the temperature/enthalpy change to be accomplished in each heat exchanger.
The enthalpy of steam at a certain pressure within the turbine is easily calculated once the expansion line is available, as explained in previous sections, and the mass flow rate of feedwater is deduced from the specific work of the turbine and the target power output of the unit. Hence, the only unknown left to be solved is how much the temperature of feedwater must be increased across each feedwater heater. This is easily optimised with the simple rule provided by Haywood [9] which suggests that the total temperature rise from condenser outlet to saturation temperature at the steam generator be divided evenly amongst all feedwater heaters plus the economiser.

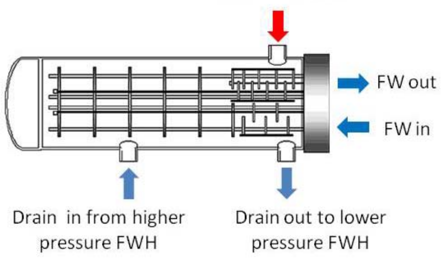

Figure 4. Characteristic temperatures of a FWH.

Once the temperature increase at each preheater is selected, extraction pressures are deduced from the Terminal Temperature Differences (TTD)[1]:

$$TTD_{FWH} = T_{sat}(p_{ext}) - T_{FWH,out} \quad \text{Eq. (8)}$$

The closure to temperature definition in the train of feedwater heaters is the application of a design Drain Cooler Approach (DCA) to each preheater:

$$DCA_{FWH} = T_{drain,out} - T_{FW,in} \quad \text{Eq. (9)}$$

The application of mass and energy conservation to each feedwater heater allows calculating steam extraction rates at the turbine and, in general, all the mass flow rates in the preheating section.

4.2. Leakages flows

Leakages of steam at different locations of the plant (turbine shaft-ends, HP turbine valve-stems, governing stage disc) are conducted to feedwater heaters or re-injected into a turbine section, where they are considered external flows. This means that they are added to the mass and heat balances around these components.
The flow of steam leaking from a packing (labyrinth seal) is calculated with the following expression [8]:

$$Q_{loss} = C\sqrt{p_2/v_1} \quad \text{Eq. (10)}$$

where p and v are the pressure and specific volume of steam ahead of the packing and C is a constant that accounts for the type of packing, available area for steam to leak (i.e. clearance area at the seal) and other specific features of the seal.
It is worth noting that the locations where steam leakages are to be considered are likely to be common to most heavy-duty steam turbines of similar configuration, even though the precise values of the corresponding C constants are expected to vary amongst different turbine manufacturers. Thus, the reference article provides tabulated information applicable to General Electric units that will not necessarily replicate the performance of equipments from other OEMs. Nevertheless, this is not a concern in the present paper since the unit running in the case study plant was originally supplied by GE.

5. EXTRACTION PRESSURES AT PARTIAL LOAD

The performance of steam turbines operating in off-design conditions is usually estimated with the *Law of the Ellipse* developed by A. Stodola and summarised by Cooke in [10] for the computational analysis of this type of power plants.
This law states that a multistage turbine expansion segment with several uncontrolled extraction groups and constant exhaust pressure is similar to a series of "equivalent nozzles", each one of which is analogous to an extraction group. The governing law for each nozzle is then described by the following formulae, known as of Stodola's ellipse [7,10]:

$$\Phi_i = \left(\dot{m}_i/\sqrt{p_i/v_i}\right) \quad \text{Eq. (11)}$$

$$\Phi_i = k\sqrt{1-(b_i/p_i)^2} \quad \text{Eq. (12)}$$

where:

- Φ_i: mass flow coefficient of any segment.
- p_i: pressure at inlet to any segment.
- T_i: temperature at inlet to any segment.

[1] Note that neither Terminal Temperature Difference nor Drain Cooler Approach apply to the Dearator.

Copyright © 2011 by ASME

- v_i: specific volume at inlet to any segment.
- b_i: pressure at exit from any segment.

This proportionality can be restated referring to a known "design point":

$$\frac{\Phi_{i,OFF}}{\Phi_{i,ON}} = \sqrt{1-\left(b_{i,OFF}/p_{,OFFi}\right)^2} \Big/ \sqrt{1-\left(b_{i,ON}/p_{i,ON}\right)^2} \qquad \text{Eq. (13)}$$

which is further simplified by algebraic rearrangement:

$$p_{i,OFF} = \sqrt{\dot{m}^2_{i,OFF} T_{i,OFF} \xi_{i,ON} + b^2_{i,OFF}} \qquad \text{Eq. (14)}$$

$$\xi_{i,ON} = \left(\frac{p_i^2 - b_i^2}{p_i^2 \Phi_i^2}\right)_{ON} \qquad \text{Eq. (15)}$$

These equations permit solving the system "backwards"; i.e. starting from the known fixed condenser pressure (which does not change in off-design operation), and calculating the extraction pressures of each group of stages upstream. This approach implies an iterative process, where the calculation of a set of flows for the uncontrolled extractions yields a new set of pressures in the following iteration.

A final consideration that must be incorporated to the calculation of part-load performance is the expected variation of turbine efficiency when working far from the design point. As stated in section 3 before, this information is usually presented in the form of efficiency vs throttle-flow ratio or pressure ratio plots, Fig. 2, where the latter parameters are the ratios of actual to nominal (design) throttle mass flow rates and pressure ratios respectively.

6. FLOW DIAGRAM OF THE MODEL

The model presented in the previous sections is integrated as sketched in Fig. 5. The set of input data comprises different aspects which can be categorised into two different groups. On one hand, information concerning plant layout: reheat or non-reheat, number and type of feedwater heaters, cross-compound or tandem-compound turbine assembly, load control system – valves, throttle, sliding pressure-,feedwater pump drive – electric or auxiliary steam turbine-. On the other hand, information concerning the operating conditions of each component of the plant: live steam pressure and temperature, condensing pressure, terminal temperature differences of the feedwater heaters and others.

All this information is used to obtain a first guess of the mass flow rate at each relevant location of the plant. Then, the steam path downstream of the turbine is analysed with the Spencer, Cotton and Canon method giving place to a first guess of the pressure, enthalpy and mass flow rate of each steam extraction. Convergence of these properties is checked then and, when reached, the heat and mass balances of the plant are obtained.

The authors' contribution to the original SCC method is mostly focused in two aspects. First, the original approach is complemented with Schegliaiev's method, namely detailed approach, thus being the user's choice which method to use. Additionally, a convergence criterion is added based on power output settings rather than live steam mass flow rate. This is particularly useful for analysing the performance of the power plant under a variety of operating conditions, as opposed to the former criterion which is of interest for performance tests.

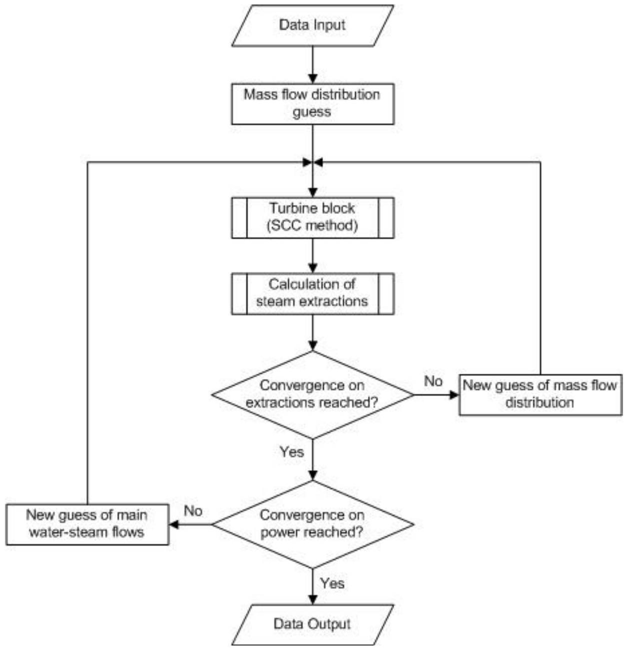

Figure 5. Block-diagram of the computational model.

7. REFERENCE PLANT

The previous sections of this article have briefly described the methodology to calculate the expected performance of steam power plants. This method is now applied to a real coal power plant located in the South of Spain, whose most relevant information is displayed in Table 2.This reference utility is a coal power plant with a rated power output of 565 MW. Live steam conditions are 168 bar and 540 ºC and the condenser operates at a rather low pressure of 65 mbar. The condenser is of the open-loop type and is cooled by sea water, thanks to the advantageous location of the plant, just one hundred metres from the sea shore.

Operating since	1985
Fuel	Bituminous coal
Net power [MW]	565
Net Heat Rate [kJ/kWh]	9473
Shaft speed [rpm / Hz]	3000 / 50
Boiler capacity [t/h]	1831
Live steam pressure [bar]	168
Live steam temperature [ºC]	540
Condenser pressure	65 mbar
Condenser type	Open loop
Mean electricity production per year	3200 GWh/year

Table 2. Main data of reference power plant.

According to the cycle layout shown in Fig. 2, the plant

Copyright © 2011 by ASME

incorporates a single reheat -hot reheat temperature is 540 ºC- and feedwater heating in seven heat exchangers, two of which operate at high pressure. The steam turbine assembly is formed by a single casing HP/IP turbine and a four flow tandem compound low pressure section with downdraft exhausts. The electric generator is air-cooled and directly driven.

8. MODEL VALIDATION

The estimated performance of the reference power plant at four different load settings (100%, 75%, 50% and 33%) is summarised in Table 3, where information regarding the mass flow rate, pressure and temperature of the most relevant states of the plant is provided. Tags are given so as to identify this information within the layout in Figure 2. The power output at step-up transformer terminals is also indicated.

		LOAD			
Tag		**100 %**	**75 %**	**50 %**	**33 %**
A	**M**	1607.0	1205.0	803.5	530.3
	P	169.8	169.8	169.8	169.8
	T	537.8	537.8	537.8	537.8
E	**M**	1452.0	1092.0	727.9	477.0
	P	42.3	31.7	21.2	14.0
	T	538.5	538.5	538.5	538.5
H	**M**	660.5	503.0	341.5	228.7
	P	12.5	9.34	6.25	4.13
	T	373.9	375.3	376.9	378.5
M	**M**	1055.0	824.9	578.4	399.1
	P	0.05	0.05	0.05	0.05
	T	0.9	0.9	0.9	1.0
AB	**M**	33.4	21.0	10.3	4.5
	P	0.25	0.19	0.13	0.10
	T	1.0	1.0	1.0	1.0
2	**M**	35.9	25.5	15.3	8.6
	P	0.59	0.44	0.30	0.20
	T	84.9	77.8	73.5	76.9
3	**M**	80.6	57.8	36.0	22.1
	P	2.22	1.67	1.11	0.73
	T	183.3	185.1	187.3	189.8
4	**M**	92.0	64.5	39.2	23.6
	P	7.40	5.55	3.70	2.44
	T	310.8	312.5	314.5	316.5
5	**M**	61.7	43.4	26.5	16.1
	P	12.50	9.38	6.25	4.13
	T	373.9	375.3	376.9	378.5
6	**M**	82.1	56.9	34.3	20.6
	P	23.10	17.33	11.56	7.62
	T	453.6	454.4	455.5	456.4
7	**M**	122.9	83.5	48.4	27.9
	P	42.31	31.73	21.16	13.96
	T	345.2	315.9	291.3	275
Power @ SUT (kW)		564763	438135	295454	193387

Table 3. Estimated plant performance at different load settings (M [kg/s], p [bar], T [ºC]).

The information in Table 3 is compared with the heat and mass balance diagrams available at the plant. These diagrams were developed originally by the firm that engineered the plant and are based on OEMs' data. They are hence useful for the purpose of validating the accuracy of the model (within the margin brought about by plant degradation). To this end, the percentage difference between the estimated performance parameters and the values reported in the heat and mass balances are presented in Table 4, where the bigger deviations are found in those points whose performance has been simplified in the model with respect to the real plant. For instance, even though condenser pressure decreases moderately with power output, a constant LP turbine exhaust pressure constraint has been imposed upon the model to facilitate the application of SCC's method.

		LOAD			
Tag		**100 %**	**75 %**	**50 %**	**33 %**
A	**M**	0.00%	2.38%	1.39%	-2.03%
	P	0.00%	-1.74%	-0.82%	-0.41%
	T	0.00%	-0.22%	-0.09%	-0.06%
E	**M**	-0.65%	1.32%	-0.74%	-5.28%
	P	0.95%	2.59%	0.00%	-4.76%
	T	0.00%	0.04%	0.04%	-0.22%
H	**M**	2.29%	4.73%	4.56%	2.83%
	P	0.00%	-0.21%	-1.73%	-4.18%
	T	0.51%	-0.03%	1.07%	0.11%
M	**M**	2.95%	6.56%	7.23%	6.20%
	P	-7.41%	8.70%	16.28%	35.14%
	T	0.00%	0.00%	0.00%	11.11%
AB	**M**	26.52%	16.67%	10.75%	4.65%
	P	13.64%	5.56%	0.00%	11.11%
	T	0.00%	0.00%	0.00%	0.00%
2	**M**	-14.52%	-1.92%	-14.04%	-23.89%
	P	5.36%	4.76%	3.45%	0.00%
	T	1.43%	-0.89%	-5.65%	0.79%
3	**M**	-2.07%	-1.53%	-4.26%	-7.53%
	P	6.73%	7.05%	0.91%	-2.67%
	T	-7.84%	-4.83%	-11.15%	-6.87%
4	**M**	-0.65%	-0.92%	-2.73%	-6.72%
	P	6.63%	5.92%	2.49%	-0.41%
	T	-2.78%	-3.43%	-3.53%	-2.91%
5	**M**	-3.14%	1.40%	-0.15%	-5.57%
	P	3.22%	2.96%	0.64%	-2.13%
	T	0.54%	0.03%	1.10%	0.13%
6	**M**	23.64%	32.02%	30.42%	10.75%
	P	6.65%	6.65%	3.12%	-1.17%
	T	-1.39%	-1.75%	-1.87%	-2.31%
7	**M**	0.66%	1.09%	1.47%	-11.43%
	P	3.09%	4.17%	0.91%	-3.92%
	T	1.14%	-3.51%	-7.26%	-10.01%
Power @ SUT (kW)		1.82%	7.44%	8.85%	6.19%

Table 4. Percentage deviations of model from original heat and mass diagrams.

In any case, estimated pressures and temperatures match real operating data with satisfactory accuracy (within the scope of the model) and it is mass flow rates which depart from the expected performance more notoriously. Additionally, a mismatch between real and estimated power output is found at low power settings, which is considered to be caused by the uncertainty in the electrical performance of generator and step-up transformer.

In spite of these differences, a global appraisal of Table 4 confirms that the accuracy of the model is globally satisfactory

 Copyright © 2011 by ASME

and it can therefore be used to assess the performance of the plant in a wide range of operating conditions. Even though the numerical results cannot be trusted for a precise numerical analysis at low power outputs, where deviations of up to 10% might be found, the model is still valid to predict performance trends under a variety of situations of interest. Moreover, in spite of the high deviations observed in some streams, for instance tags AB and 6 in Table 4, it must be noted that these translate into mass flow rates differences of 7 and 15 kg/s at full load with respect to the corresponding values in Table 3, which represent 0.4 and 0.9 percent of the live steam flow (tag A). This is shown in the following sections.

Finally, the estimated expansion lines are plotted in Fig. 6 for the four cases considered in Tables 3 and 4. As mentioned before, a reduction in power output is expected to shift the expansion lines rightwards due to the increased pressure drop at the control valves and the efficiency drop of the high pressure section. On the contrary, for the remaining stages in the high pressure section and the entire IP and LP sections, parallel expansion lines indicate a rather constant efficiency regardless of unit load, Fig. 2. Part load operation also yields a reduction of moisture in the low pressure turbine exhaust.

Finally, the estimated expansion lines are plotted in Fig. 6 for the four cases considered in Tables 3 and 4. As mentioned before, a reduction in power output is expected to shift the expansion lines rightwards due to the increased pressure drop at the control valves and the efficiency drop of the high pressure section. On the contrary, for the remaining stages in the high pressure section and the entire IP and LP sections, parallel expansion lines indicate a rather constant efficiency regardless of unit load, Fig. 2. Part load operation also yields a reduction of moisture in the low pressure turbine exhaust.

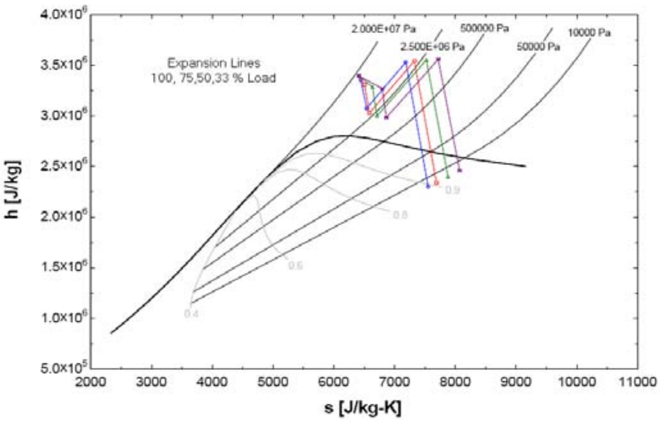

Figure 6. Estimated expansion lines for different steam turbine loads (100%, 75%, 50%, 33%).

9. ANALYSIS OF RESULTS

9.1. Variable terminal temperature difference of a feedwater heater

The modification of Terminal Temperature Differences at the feedwater heating train affects the performance of the entire power plant as reported by Alconchel et al. in [11]. For instance, let us assume that the TTD of a particular feedwater heater were to be voluntarily increased (i.e. not as a result of fouling or other undesirable phenomenon). This would imply a decrease in the temperature of feedwater leaving the component and a reduction in the mass flow rate of steam extracted from the turbine. A higher steam flow rate would then expand in the turbine downstream of the aforementioned extraction port, raising the backpressure of the remaining lower pressure stages. This increase in pressure would automatically imply a similar increase in the corresponding saturation temperature at the preheater and, therefore, in the temperature of feedwater leaving the heat exchanger.

In summary, feedwater temperature would initially be expected to decrease and, later, to increase again. The first effect is usually dominant and, therefore, feedwater temperature decreases.

Taking a look at the lower pressure heaters, whose TTDs remain constant but whose operating pressures and therefore saturation temperatures have increased, they would in turn increase the mass flow rate of steam bled from the turbine, partly compensating for the aforementioned effect. These cascade effects are attenuated for feedwater heaters far from the modified component (heat exchanger where TTD is increased).

Higher pressure heaters would similarly experience an increase in extraction mass flow rate if TTD is to be maintained, since the feedwater coming from the upstream (lower pressure) heaters is at a lower temperature. This higher extraction rate reduces the pressure of the turbine downstream of the corresponding extraction port, thus counteracting in part the effect described in the first paragraph of this section.

		TTD increases 2ºC in FWH_i					
		FWH_1	FWH_2	FWH_3	FWH_4	FWH_6	FWH_7
FWH_1	M	-6.41	0.05	0.15	0.02	-0.02	0.71
	P	0.02	0.03	0.09	0.02	0	0.40
FWH_2	M	10.92	-12.10	0.10	0.01	-0.03	0.57
	P	-0.29	0.03	0.09	0.02	0	0.43
FWH_3	M	0.16	4.65	-14.50	0.07	-0.03	0.55
	P	-0.03	-0.32	0.10	0.02	0	0.44
FWH_4	M	0.02	0.19	10.00	-5.35	-0.04	0.59
	P	0	-0.04	-0.80	0.027	-0.01	0.45
FWH_6	M	0.01	0.02	0.23	0.17	-7.08	0.85
	P	0	-0.01	-0.10	-0.07	-0.01	0.46
FWH_7	M	0	0.01	0.08	0.06	4.62	-5.91
	P	0	0	-0.02	-0.03	-0.29	0.48

Table 5. Effect of increasing the TTD of FWH_i by 2ºC on the remaining feedwater heating section[2] (figures indicate percentage variation with respect to design values).

Table 5 shows the effect of increasing TTD in a single feedwater heater on the performance of the remaining preheaters. Changes in pressure and mass flow of steam are provided for the reference plant operating at full capacity; all

[2] Following the standard notation, FWH_1 and FWH_7 are the lowest and highest pressure feedwater heaters.

 Copyright © 2011 by ASME

figures are shown in percentage difference with respect to their corresponding rated values.
The effect of changing TTD of one feedwater heater on its own demand for bled steam is marked in grey in the main diagonal of Table 5. As mentioned earlier, a reduction in steam mass flow rate should be expected due to the lower feedwater delivery temperature required. Other than that, no significant impact on other feedwater heater's performance is observed when TTD is changed in a single component.

9.2. Variable drain cooler approach of a feedwater heater

Modifications of the Drain Cooler Approach of one feedwater heater are expected to impact the performance of the remaining preheaters as well [8,11]. For instance, increasing the DCA in FWH_i increases the mass flow rate of steam that needs to be bled from the turbine, in order to compensate for its lower enthalpy drop (in the assumption that feedwater inlet temperature remains constant). This brings about a reduction in the amount of steam flowing through the turbine downstream of the extraction port under analysis, thus reducing the pressure at the remaining turbine ports feeding the lower pressure preheaters (FWH_1 to FWH_{i-1}).
At the same time, the drains from FWH_i are at a higher temperature and, hence, when conducted to the immediate lower pressure preheater located upstream (FWH_{i-1}), a reduction in mass flow rate extracted from the turbine is found. This secondary effect partly offsets the previous one and attenuates the reduction of turbine internal flow and pressure.
With respect to the higher pressure FWHs, the reduction in extraction pressure along with the constant TTDs yield a lower feedwater delivery temperature at the feedwater heater where DCA has been modified. As a result, the mass flow rate of steam required at the downstream (higher pressure) preheater is expected to increase.

		DCA increases 5ºC in FWH_i					
		FWH_1	FWH_2	FWH_3	FWH_4	FWH_6	FWH_7
FWH_1	M	3.56	-2.97	0.02	0.01	0.02	0
	P	0	0.01	0.01	0.01	0.01	-0.22
FWH_2	M	0.21	5.06	-4.50	0.09	0.01	-0.01
	P	-0.05	-0.14	0.01	0.01	0.01	0
FWH_3	M	0.03	0.07	1.70	-1.06	0.01	-0.01
	P	-0.01	-0.02	-0.12	0.01	0.01	0
FWH_4	M	0.00	0.01	0.07	0.78	0.01	-0.01
	P	0	0	-0.02	-0.06	0.01	0
FWH_6	M	0	0	0.01	0.02	2.07	-1.52
	P	0	0	0	-0.01	-0.09	0
FWH_7	M	0	0	0	0.01	0.07	1.08
	P	0	0	0	0	-0.03	-0.06

Table 6. Effect of increasing the DCA of FWH_i by 5ºC on the remaining feedwater heating section (figures indicate percentage variation with respect to design values).

Both effects of a change of DCA in FWH_i on the performances of FWH_{i-1} and FWH_{i+1} are observed in Table 6. For instance, when FWH_3's DCA is modified, the mass flow rates of FWH_2 and FWH_4 experience modifications of -4.5% and 0.07% respectively. This pattern is followed by all feedwater heaters except FWH_5, which is the deareator.

9.3. Feedwater heater out of service

One of the most usual abnormal operations in heavy-duty steam power plants is to put one or more feedwater heaters off-service. This situation is likely to be found during maintenance or cleaning works performed to prevent heat exchanger effectiveness from decaying. It is worth noting that an incorrect maintenance of this equipment would inevitably lead to an increase of TTD and DCA (though in this case not due to a change in the mass flow rate of steam extracted from the turbine, as it was the case in the previous sections).
Since these labours are done regularly, only rarely is the plant stopped to carry them out. On the contrary, it is common to bypass the component where works have to be done, keeping the plant in operation even though efficiency and power output are bond to decrease with respect to their rated values.
When a heater is bypassed, trying to maintain the TTD of the remaining FWHs automatically increases the extraction flows at the downstream (higher pressure) heaters. Two different situations can then take place. At high loads, 75-100%, these operating conditions imply unpractical volumetric steam flows in the extraction lines and feedwater heaters, which are usually designed for a maximum continuous volumetric flow rate of 115% with respect to their rated values. The downstream terminal temperature differences are then permitted to increase even though cycle efficiency is further reduced.
The limitation of maximum volumetric flow rate is not violated at low power settings. However, TTD is likely to increase to avoid unbalanced extraction flows between feedwater heaters upstream and downstream of the equipment that is out of service.
These considerations are summarised in Table 7 for the power plant under analysis running at full capacity. Let us analyse the case where FWH_3 is put out of service for maintenance. Table 7 shows that the downstream heaters, FWH_4-FWH_7, demand a much higher extraction flow (around 15% higher) now due to the need to compensate feedwtater temperature for the missing FWH_3. This in turn reduces turbine pressure in the first segments, what manifests in Table 7 as an extraction pressure reduction for FWH_4-FWH_7.
FWH_1 and FWH_2 experience moderate increases in bled steam pressure and mass flow rate. The reason for the higher pressure is that, even though the mass flow rate of steam expanding in the turbine is significantly reduced in the first stages before the extraction port for FWH_3, these higher extraction flows do not offset the increase in turbine flow brought about by the disablement of FWH_3. Globally, the mass flow rate of steam flowing downstream of the port for FWH_3 is therefore increased and so is pressure.
The effect on power output of an out-of-service feedwater heater is not uniform. Instead, even if in all cases efficiency

 Copyright © 2011 by ASME

drops by around 1% with respect to its rated value, power output shows a linear evolution from a rather negative effect when FWH_1 is disabled to a rather positive effect when FWH_7 is off-work. These opposite effects are mostly connected with the mass flow rate and pressure of steam expanding in the turbine. Hence, when the feedwater heater that is put out of service is close to the steam generator, FWH_6 and FWH_7, the total mass flow flowing through the turbine increases and brings about a higher pressure along the entire expansion line. This translates into a higher than rated power output, despite the lower efficiency.

On the contrary, when the disabled heater is close to the condenser, the higher extraction flows in the remaining heaters reduces turbine pressure. Accordingly, power output and efficiency are reduced.

		FWH_i out of service					
		FWH_1	FWH_2	FWH_3	FWH_4	FWH_6	FWH_7
FWH_1	M	0	0.68	3.84	6.58	7.14	12.16
	P	0	0.42	2.38	4.00	4.05	6.72
FWH_2	M	13.78	0	3.29	5.55	5.55	9.78
	P	-4.01	0	2.55	4.28	4.35	7.20
FWH_3	M	14.67	14.48	0	5.88	5.25	9.44
	P	-4.35	-2.47	0	4.38	4.49	7.37
FWH_4	M	14.35	14.32	14.85	0	5.52	10.14
	P	-3.23	-1.64	-3.49	0	4.50	7.51
DA	M	14.02	8.37	13.84	14.17	7.52	13.75
	P	-2.37	-0.87	-3.04	-0.18	4.56	7.63
FWH_6	M	14.83	0.68	12.90	13.63	0	14.71
	P	-1.54	-0.30	-2.34	-1.50	0	7.83
FWH_7	M	3.63	0.24	14.74	14.10	13.82	0
	P	-0.67	-0.10	-1.55	-1.27	0.61	0
Output	MW	-3.21	-0.46	-0.27	1.31	2.37	4.75
η	%	-1.49	-0.47	-1.49	-1.47	-1.08	-0.91

Table 7. Effect of disabling FWH_i on the remaining feedwater heating section (figures indicate percentage variation with respect to design values).

Regarding Table 7, it is worth noting that the particular FWH_i for which power output does not decrease anymore and starts to increase (FWH_4 in Table 7) depends on two factors: load and overflow capacity. Thus, depending on the values of these two parameters, the transition FWH_i might shift towards the condenser or towards the steam generator. Nevertheless, in all cases, putting FWH_1 out of service always has a negative impact on power output.

10. CONCLUSIONS.

The main conclusions of this work are:

- With respect to the model of performance based on the Spencer, Cotton and Cannon method, good agreement has been found when comparing real and estimated performances of a coal power plant located in the South of Spain. Even if deviations between estimates and original heat and balance diagrams data available at the plant exist and increase at part load, it is concluded that the model is reliable for predicting the performance of power plants with similar characteristics (within a margin lower than 10% for the global performance parameters).
- Increasing the Terminal Temperature Difference in a feedwater heater brings about a reduction of its extraction mass flow rate and, in turn, increases the demand of steam from the turbine for the feedwater heater immediately upstream (higher pressure). This is due to the lower inlet temperature of feedwater in the latter heat exchanger.
- Increasing the Drain Cooler Approach in a feedwater heater increases the demand of steam from the turbine to compensate for its lower enthalpy drop at the heat exchanger. At the same time, minimum increase and moderate decrease of the bled steam mass flow rates for the feedwater heaters located immediately downstream and upstream of the modified heater take place. The effect of modifying Drain Cooler Approaches is nevertheless less significant than that observed when Terminal Temperature Differences are changed.
- Disabling one feedwater heater for maintenance works affects efficiency negatively.
- However, the effect of this abnormal operation on power output depends on which heater is put out of service. It is observed that power output increases when the bypassed heater is of the high pressure type, i.e. close to the steam generator and far from the condenser. On the contrary, when the bypassed heater is located at the other end of the feedwater heating train, low pressure section close to the condenser, power output is reduced.
- In between these two extreme cases, a linear evolution is observed. The precise feedwater heater for which power output stops decreasing and starts to increase depends on the load of the plant and the particular design of the feedwater heater.

Overall, the model of performance presented in this work provides the authors with a useful tool to assess plant performance under unusual/abnormal operation, even if the numerical information might deviate from the real performance by a margin that narrows down for loads higher than 50-60%. More in detail, robustness, flexibility, ease-of-use and short computational time are interesting features of the software developed.

NOMENCLATURE

A_{an}	Last stage annulus area [m^2]
b	Pressure at exit from turbine segment [bar]
DCA	Drain cooler approach [ºC]
ELEP	Expansion line end point [kJ/kg]
FWH	Feedwater heater
Gen_{loss}	Generator loss [kW]
h	Enthalpy [kJ/kg]
MVA	Generator capability [MVA]
MW	Generator output [MW]
N	Number of parallel expansion paths
NV	Number of control valves
OEM	Original Equipment Manufacturer
ON	on-design / rated

Copyright © 2011 by ASME

OFF	off-design / part load
p	Pressure [bar]
PD	Pitch diameter of governing stage [m]
PF	power factor [-]
Q	Mass flow rate [kg/s]
Q_v	Mass flow rate at beginning of expansion [kg/s]
s	Entropy [J/kg ºC]
T	Temperature [ºC]
Th	Throttle conditions
TFR	Throttle flow ratio
TTD	Terminal temperature difference [ºC]
SUT	Step-up transformer
UEEP	Used energy end point [kJ/kg]
V	Specific volume [m^3/s]
Y	Humidity [-]
W	Specific work [kJ/kg]
Δh	Isentropic enthalpy drop [kJ/kg]
Φ	Mass flow coefficient of a turbine segment

REFERENCES

[1] G.B. Warren, P.H. Knowlton Jr., *Relative Engine Efficiencies Realizable From Large Modern Steam Turbine-Generator-Units*, Trans. ASME, 1941, vol. 63, p.125.

[2] C.W. Elston, P.H. Knowlton Jr., *Comparative Efficiencies of Central-Station Reheat and Nonreheat Steam-Turbine Generator Units,* Trans. ASME, 1952, vol. 74, 1389.

[3] H. Hegetschweiler, R.L. Bartlett, *Predicting Performance of Large Steam Turbine-Generator Units for Central Stations*, Trans. ASME, 1957, vol. 79, 1085.

[4] R.C. Spencer, K.C. Cotton, C.N. Cannon, *A Method for Predicting the Performance of Steam Turbine-Generator Unit 16,500 kW and Larger*, ASME Paper 62-WA-209.

[5] K.C. Cotton, *Evaluating and Improving Steam Turbine Performance*, 2nd Ed., Cotton Fact Inc., Rexford, 1998.

[6] A.V. Schegliaiev, *Steam Turbines*, Spanish Edition, Ed. Mir, Moscow, 1978.

[7] A. Stodola, *Steam and Gas Turbines*, McGraw-Hill, 1927, New York.

[8] L.F. Drbal (ed.), *Power Plant Engineering*, Springer, 1996, New Yotk.

[9] R.W. Haywood, *Analysis of Engineering Cycles (2nd Ed.),* Pergamon Press, 1975, Oxford.

[10] D.H. Cooke, *Modeling of off design multistage turbine pressures by Stodola's ellipse*, presented at Energy Incorporated Pepse users' group meeting, 1983, Richmond.

[11] J.A. Alconchel, A. Valero, J. Abadía, *Exergy Simulation of Real Operating Power Plants*, Proc. Thermoeconomic Analysis of Improvement of Energy Systems, 1989, Beijing.

APPENDIX

The correction factors CF in Table 1 can be analytically calculated with the polynomials in Table A1 where the coefficients A_{ij} not listed are null:

$$\Delta\eta(\%) = \sum_{i=0}^{n_1}\sum_{j=0}^{n_2} A_{ij} X_1^i X_2^j \quad \text{Eq. (A1)}$$

$$TFR = Q_{th,actual}/Q_{th,ON} \quad \text{Eq. (A2)}$$

Table A2 provides the polynomials needed to calculate the electrical losses where:

$$K_1 = \sum_{i=0}^{n} A_i MVA_{rated}^i \quad \text{Eq. (A3)}$$

$$K_2 = \sum_{i=0}^{n} A_i \left(100 \cdot \left(\frac{MW_{actual}}{PF}\right)/MVA_{rated}\right)^i \quad \text{Eq. (A4)}$$

CF#	*Y*	X_1 / X_2	Coefficients	
6	$\Delta\eta$	$\frac{P_{XD}}{P_T}$ $ln\left(\frac{0.45392 \cdot Q_v}{3600}\right)$	A_{00}=11.151 A_{01}=-0.50091	A_{10}=-63.0 A_{11}=2.83
7	$\Delta\eta$	*PD*/0.3048	A_0=4.37	A_1=-0.115
8	$\Delta\eta$	*TFR* *PD*/0.3048	A_{00}=-21.8085 A_{01}=0.573908	A_{10}=21.8085 A_{11}=-0.573908
9	$\Delta\eta$	*TFR* $ln\left(\frac{P_{Th}}{b_{ON}}\right)$	A_{00}=-60.75 A_{01}=17.50 A_{10}=66.85 A_{20}=29.75	A_{30}=-35.85 A_{11}=-20.02 A_{21}=-0.525 A_{31}=3.045
10	$\Delta\eta$	$\frac{b_{ON}}{P_{Th}}$ $ln\left(\frac{0.45392 \cdot Q_v}{3600}\right)$	A_{00}=25.665 A_{01}=-1.33281	A_{10}=-145.0 A_{11}=7.53
11	$\Delta\eta$	*1-TFR* $\frac{P_{Th}}{b_{ON}}$	A_{10}=42.676909 A_{20}=-89.391147 A_{30}=9.0376638 A_{11}=-26.221836 A_{21}=25.549385 A_{31}=8.8283868	A_{12}=4.047955 A_{22}=-1.4725197 A_{32}=-4.0183332 A_{13}=-0.14502211 A_{23}=-0.18580363 A_{33}=0.42657518
12	$\Delta\eta$	*TFR* *NV*	A_{00}=-5.4 A_{01}=0.45	A_{10}=4.395 A_{11}=-0.36625
14	$\Delta\eta$	$14.5037738 \cdot P_{bowl}$ $32+1.8 \cdot T_{bowl}$	$A_{00}= -2.06230607 \cdot 10^{1}$ $A_{01}= -1.71384968 \cdot 10^{-2}$ $A_{02}= -2.91759737 \cdot 10^{-5}$ $A_{03}= 2.03664452 \cdot 10^{-8}$ $A_{04}= -3.25583716 \cdot 10^{-12}$ $A_{10}= 6.96400731 \cdot 10^{-2}$ $A_{20}= -8.47042456 \cdot 10^{-5}$ $A_{30}= 4.71274876 \cdot 10^{-8}$	$A_{40}= -1.01713246 \cdot 10^{-11}$ $A_{11}= -1.11624068 \cdot 10^{-5}$ $A_{21}= 4.71368174 \cdot 10^{-8}$ $A_{12}= 1.17715642 \cdot 10^{-7}$ $A_{22}= -1.50002390 \cdot 10^{-10}$ $A_{13}= -4.66856314 \cdot 10^{-11}$ $A_{31}= -1.77537825 \cdot 10^{-11}$ $A_{23}= 5.67898991 \cdot 10^{-14}$ $A_{32}= 4.99892414 \cdot 10^{-14}$ $A_{33}= -1.89101928 \cdot 10^{-17}$

Table A1. Polynomials to calculate the correction factors in Table 1.

Type	*Y*	*X*	Coefficients
Conventional cooling 3600 rpm	K_1	MVA_{rated}	A_0=1.5944523 $A_1=-1.18 \cdot 10^{-2}$ $A_2=1.114 \cdot 10^{-4}$ $A_3=-4.71 \cdot 10^{-7}$ $A_4=6.948 \cdot 10^{-10}$
	K_2	$100\frac{\left(\frac{MW_{actual}}{PF}\right)}{MVA_{rated}}$	A_0=5.32849 $A_1=-1.92 \cdot 10^{-1}$ $A_2= 3.18 \cdot 10^{-3}$ $A_3=-2.09 \cdot 10^{-5}$ $A_4=4.091 \cdot 10^{-8}$
Hydrogen cooling 3600 rpm	K_1	MVA_{rated}	A_0=1.51095 $A_1=-1.11 \cdot 10^{-3}$ $A_2=1.49 \cdot 10^{-6}$ $A_3=-8.40 \cdot 10^{-10}$ $A_4=1.697 \cdot 10^{-13}$
	K_2	$100\frac{\left(\frac{MW_{actual}}{PF}\right)}{MVA_{rated}}$	A_0=4.543015 $A_1=-2.02 \cdot 10^{-1}$ $A_2=4.35 \cdot 10^{-3}$ $A_3=-4.18 \cdot 10^{-5}$ $A_4=1.499 \cdot 10^{-7}$

Table A2. Polynomials to calculate generator losses.

Copyright © 2011 by ASME